Carbon-ion Evokes Metabolic Reprogramming and Individualized Response in Prostate Cancer

Yulei Pei

Department of Radiation Oncology, Shanghai Proton and Heavy Ion Center, Fudan University Cancer Hospital, Shanghai 201321, China; Shanghai Key Laboratory of Radiation Oncology (20dz2261000); Shanghai Engineering Research Center of Proton and Heavy Ion Radiation Therapy, Shanghai 201321, China.

Renli Ning

Department of Research and Developement, Shanghai Proton and Heavy Ion Center, Fudan University Cancer Hospital, Shanghai 201321, China; Shanghai Key Laboratory of Radiation Oncology (20dz2261000); Shanghai Engineering Research Center of Proton and Heavy Ion Radiation Therapy, Shanghai 201321, China

Ping Li

Department of Radiation Oncology, Shanghai Proton and Heavy Ion Center, Shanghai 201321, China; Shanghai Key Laboratory of Radiation Oncology (20dz2261000); Shanghai Engineering Research Center of Proton and Heavy Ion Radiation Therapy, Shanghai 201321, China.

Wei Hu

Department of Radiation Oncology, Shanghai Proton and Heavy Ion Center, Fudan University Cancer Hospital, Shanghai 201321, China; Shanghai Key Laboratory of Radiation Oncology (20dz2261000); Shanghai Engineering Research Center of Proton and Heavy Ion Radiation Therapy, Shanghai 201321, China

Yong Deng

Department of Research and Developement, Shanghai Proton and Heavy Ion Center, Shanghai 201321, China; Shanghai Key Laboratory of Radiation Oncology (20dz2261000); Shanghai Engineering Research Center of Proton and Heavy Ion Radiation Therapy, Shanghai 201321, China

Zhengshan Hong

Department of Radiation Oncology, Shanghai Proton and Heavy Ion Center, Shanghai 201321, China; Shanghai Key Laboratory of Radiation Oncology (20dz2261000); Shanghai Engineering Research Center of Proton and Heavy Ion Radiation Therapy, Shanghai 201321, China

Yun Sun

Department of Research and Developement, Shanghai Proton and Heavy Ion Center, Shanghai 201321, China; Shanghai Key Laboratory of Radiation Oncology (20dz2261000); Shanghai Engineering Research Center of Proton and Heavy Ion Radiation Therapy, Shanghai 201321, China.

Xiaomao Guo

Department of Research and Development, Shanghai Proton and Heavy Ion Center, Fudan University Cancer Hospital, Shanghai 201321, China; Shanghai Key Laboratory of Radiation Oncology (20dz2261000); Shanghai Engineering Research Center of Proton and Heavy Ion Radiation Therapy, Shanghai 201321,China

Qing Zhang (qing.zhang@sphic.org.cn)

Department of Research and Development, Shanghai Proton and Heavy Ion Center, Fudan University Cancer Hospital, Shanghai 201321, China; Shanghai Key Laboratory of Radiation Oncology (20dz2261000); Shanghai Engineering Research Center of Proton and Heavy Ion Radiation Therapy, Shanghai 201321,China

---

Research

Keywords: Metabolites, Prostate cancer, Carbon ion radiotherapy, Metabolic reprogramming, Individualized response, Metabolites profiles

Posted Date: June 15th, 2021

DOI: https://doi.org/10.21203/rs.3.rs-604086/v1

Abstract

Background: Carbon ion radiotherapy (CIRT) is a novel and powerful tool for prostate cancer (PCa). However, the underlying mechanism for individualized treatment response after CIRT was not clear, and there was still no effective indicator to timely demonstrate the treatment response. Metabolic reprogramming is one of the main hallmarks of malignancy. Metabolic status might have a high relationship with the radiosensitivity and the individualized radiation response. The significant changes of metabolites profiles were detected after radiotherapy in the serum sample of different malignancies. But there was limited data regarding CIRT induced metabolic changes in prostate cancer. Our aim was to preliminary investigate the carbon-ion induced metabolic reprogramming in PCa patients and the individualized response of PCa patients to carbon ion.

Methods: Urine samples collected from 15 pathology confirmed PCa patients before and after CIRT were enrolled into this analysis. High-throughput UPLC-MS/MS system was used for metabolites detection. XCMS online, MetDNA and MSDIAL were used for peak detection and identification of metabolites. Statistical analysis and metabolic pathway analysis were performed on Metaboanalyst.

Results: A total of 1701 metabolites were monitored by high-throughput UPLC-MS/MS and 217 metabolites were identified. The PCA scores plot revealed clear discrimination of the patient's urine metabolites profiles before (pre-CIRT) and after (pre-CIRT) CIRT treatment. 35 metabolites significantly altered after CIRT, and these metabolites mainly were amino acid. Pathway enrichment analysis further identified these metabolites could be enriched in 8 pathways (FDR<0.05, impact>2), while arginine biosynthesis and histidine metabolism pathways were the most significant. In addition, the HCA shows that after CIRT, the patients can be clustered into two groups according to the metabolites profiles. The discriminatory metabolites after CIRT in patients urine mainly enriched in the pathway of arginine biosynthesis and phenylalanine, tyrosine, and tryptophan biosynthesis.

Conclusion: Metabolic reprogramming and metabolic inhibition seems one of the most important mechanisms of CIRT to cure PCa. Urine metabolites also showed their potentials to timely identify the individualized response of PCa patients to CIRT.

Background

CIRT is a novel and powerful tool for radiotherapy and has gradually been recognized as one of the best strategies for PCa with the reported excellent five-year biochemical recurrence-free survival (RFS) and a favorable level of late gastrointestinal and genitourinary toxicities due to its inspiring physical and biological advantages [1, 2]. In the past seven years, Shanghai Proton and Heavy Ion Center (SPHIC), as the first carbon-ion treatment center in China, has treated 162 pathology confirmed PCa patients and the 3 years BFS reached 93% under CIRT. However, these PCa patients showed an individualized treatment response after carbon ion irradiation, and the underlying mechanism was not clear until now. Moreover, there was still no effective indicator to timely demonstrate the treatment response. Patients might wait

several months for the serum total PSA and MRI results after the completion of irradiation, which adversely impacts decision-making. Exploring the underlying mechanism and finding timely and powerful tools would add value to early evaluate the prognosis of PCa patients treated with CIRT.

Metabolic reprogramming is one of the main hallmarks of malignancy, in which tumor cells make metabolic disorders to promote their growth and proliferation, as well as other components like microenvironment and immune cell. Metabolic reprogramming was also detected to have the potential to produce an immunosuppressive metabolic microenvironment which is conducive to tumor proliferation and escapes [3]. Data further showed that metabolic status might have a high relationship with the radiosensitivity and the individualized radiation response [4]. The significant changes of metabolites profiles were detected after radiotherapy in the serum samples of different malignancies such as hepatocarcinoma and breast cancer [5, 6]. Moreover, carbon ion has been proved to produce different metabolic status when compared to photon [7]. But the CIRT induced metabolic changes of prostate cancer were largely unknown.

Furthermore, one pilot study from Poland evaluated the free amino acid profiles in both prostate patients' serum and urine samples and tried to find a better biomarker other than PSA in order to improve the sensitivity and specificity for prostate cancer diagnosis [8]. The result is interesting, it was found that the metabolites might have similar or even better performance than PSA (AUC ranging from 0.53 to 0.83) [9] for PCa detection, which indicated that metabolic changes might add value to early evaluate the treatment response after radiotherapy. Recently, limited metabolomics studies evaluated the PCa treatment response to radiation and showed that the most significant alterations after photon irradiation were linked to metabolic pathways of nitrogen, pyrimidine, purine, porphyrin, alanine, aspartate, glutamate, and glycerophospholipid [10]. In another quality-of-life photon studies, metabolomics was alternatively used to determine individualized radiation toxicities [11]. But there were lack studies that explored the carbon-ion induced metabolic reprogramming and the individualized response in PCa patients.

Our aim was to preliminary investigate carbon-ion induced metabolic reprogramming in PCa patients and individualized response of PCa patients to carbon ion. As a kind of completely non-invasive biological fluid, it contains over 2500 metabolites and allows us to observe global metabolic changes in cancer patients [12]. The discriminatory metabolites and pathways will be identified and analyzed. We expect this primary investigation of carbon-ion induced metabolic reprogramming and the individualized response of PCa patients will further step up the PCa CIRT treatment, and will also add value to either CIRT or photon radiotherapy in other malignancies.

Materials And Methods

Study samples and population

From July 2020 to December 2020, 15 patients with pathologically confirmed cTNM prostate adenocarcinoma were enrolled in this study. Radiotherapy was delivered with carbon ion beam by Siemens IONTRIS particle therapy device in Shanghai Proton and Heavy Ion Center. The clinical target volume (CTV) included the prostate with or without proximal seminal vesicles based on different risk group types. The median CIRT doses of prostate was 60.4 GyE (range 55.2–65.6 GyE) in 12–16 fractions, and was prescribed to the 99% isodose line. Risk stratification was based on NCCN guidelines version 2.2020. Demographic and clinical characteristics of enrolled patients are demonstrated in Table 1.

Table 1
Patients' demographic and clinical characteristics

Characteristics	Statistics	No of patients (n = 15)	(%)
Age (years)	73 (50–82)		
T	T1	1	6.7
	T2	9	60
	T3	4	26.7
	Tx	1	6.7
N	M0	15	100
M	N0	14	93.3
	N1	1	6.7
Gleason Score	6	7	46.7
	7	4	26.7
	≥ 8	4	26.7
Risk Group for	Low	2	13.3
Localized PCa	Intermediate	6	40
	High	5	33.3
	Very high	1	6.7
ADT, androgen-deprivation therapy.			

Samples collection and preparation

Urine samples were collected right before and after CIRT. All the samples were deposited under 4 ℃ immediately after collection. 0.22 μm membrane filters were used to remove contaminated bacteria from urine samples before stored at -80 ℃. All urine samples were thawed at room temperature on ice. 800 μl chilled methanol/acetonitrile (1:1, v/v) was add to 200 μl samples. The mixture was vortexed for 30 sec, sonicated for 10 min, incubated for 1 hour at − 20 ℃ and then centrifuged at 13000 g for 15 min at 4°C.

Afterwards, the supernatant was transferred into a new Eppendorf tube and evaporated in Integrated Vacuum Concentrator (SpeedVac SPD1030). Evaporated dry supernatant was kept at -80 ℃ until analyzed. Dry supernatant was re-dissolved in 200 µL chilled acetonitrile/water (1:1, v/v), vortexed for 30 sec, sonicated for 10 min, centrifuged at 12 000 g for 15 min at 4 ℃, and then new supernatant was transferred into sampler vials. Quality control (QC) samples were prepared by mixing equal amounts (50 µL) of each sample.

High-throughput UPLC -MS/MS analysis

High-throughput UPLC-MS/MS analysis of urine samples was performed on AB SCIEX ExionLCY system combined with AB SCIEX 500R QTOF. We separated urinary metabolites in ACQUITY UPLC BEH Amide 1.7 µm (2.1 mm × 100 mm) column. Autosampler and column temperatures were set at 4°C and 40°C, respectively. The injection volume was 1 µL and the flow speed was 0.3 ml/min. Mobile phases A was water with 10 mM NH4FA and 0.1%FA, and mobile phases B was acetonitrile: methanol = 95:5 (V/V)with 10 mM NH4FA and 0.1%FA. 17 min gradient was described as follows: 2 min, 100% B; 11 min, 45% B; 12 min, 45% B; 12.1 min, 100% B; 17 min, 100% B. Full MS was acquired using scans from 50 to 1000 m/z Da in the TOF MS mode. Electrospray ionization mode was performed in the mass spectrometry analysis. The following electrospray ionization (ESI) parameters were selected: Ion source gas 1: 55 psi, Ion source gas 2: 55 psi; T: 550℃; Spray voltage: 5500 V (+); TOF MS Collision energy: 10 V, TOF MSMS Collision energy: 35 ± 15 V. The order of sample analysis was randomized and the QC sample was analyzed every 10 injections. 3 blanks and 6 replicates of the QC sample were injected at the beginning of batch for column conditioning. The sample set included 3 blanks, 9 QC sample and 30 urine samples. Autocalibration was performed every 5 analysis.

Data collection and metabolites dentification

The raw data was acquired by UPLC -MS/MS and the file format was conversed using MSconvert software and Analysis Base File Converter. Conversed data files were processed by MSDIAL for identification. Upload MSconvert software conversed data onto XCMS online for peak detection and alignment. The parameters were set as ppm = 30, minimum peak width = 10, maximum peak width = 30, Signal/Noise threshold = 6, mzdiff = 0.01, mzwid = 0.025. Peak table were uploaded onto MetDNA for the dentification of metabolites. Upload the acquired peak table to Metaboanalyst for statistical analysis and metabolic pathway analysis. Concentrations of metabolites were represented by peak area and normalized by data of creatinine.

Analysis

MetaboAnalyst 5.0 was used to select the metabolites statistically significant differences between pre-CIRT samples and post-CIRT samples, performed by volcano plot, which is combination of fold change (FC) analysis and non-parametric tests. False discovery rates (FDR) were calculated to reduce the incidence of false-positives. Unsupervised principal component analysis (PCA) was performed to detect the significant separation shift between compared groups. Supervised multivariate analysis, partial least-squares discriminant analysis (PLS-DA), was performed to achieve maximum separation among the

groups. Sparse PLS-DA (sPLS-DA) algorithm was used to reduce the number of variables (metabolites) to produce robust and easy-to-interpret models. Hierarchical cluster analysis (HCA) was used to separate the metabolites profiles between compared groups. Boxplots were used to show changes in urine metabolite concentrations from PCa patients showed the minimum, lower quartile, median, upper quartile, and maximum values of concentrations of metabolites.

Results

CIRT treatment significantly altered the urine metabolites profiles in PCa patients

A total of 1701 metabolites were monitored by UPLC-MS/MS and 217 metabolites were identified. Multivariate analysis was performed using PCA, PLS-DA and sPLS-DA. All samples were analyzed with the unsupervised model PCA to examine possible sample group separations and sample clustering behavior. The PCA scores plot reveals clear discrimination of the patient's urine metabolites profiles before (pre-CIRT) and after (pre-CIRT) CIRT treatment (Fig. 1a-c). Pre-CIRT samples clusters on the left side of the scores plot and post-CIRT samples clusters on the right side, with a small overlap, demonstrating the significant difference of metabolites profiles before and after CIRT treatment. Moreover, HCA of metabolites can clearly discriminate the majority of pre-CIRT samples with post-CIRT samples (**Supplementary Fig. 1**). Furthermore, the heat map shown in **Fig. 2a** reveals the concentration of metabolites in the urine sample experienced down-regulation in most patients after CIRT. Volcano plot identifies 35 significantly altered metabolites after CIRT, and these metabolites mainly are amino acid (Fig. 2b). 33 of the 35 urine metabolites are down-regulated after CIRT treatment, and typical metabolites include L-Glutamate, L-Glutamine, L-Cystine, glutathione, anthranilate, 5'-Methylthioadenosine. Two urine metabolites are up-regulated, including (R)-4'-Phosphopantothenoyl-L-cysteine, betaine (Fig. 2c). The above results indicate the CIRT can significantly alter the PCa metabolism, and especially can significantly decrease the amino acid metabolism.

CIRT induced metabolic changes mainly enriched in arginine biosynthesis and histidine metabolism

We further performed pathway enrichment analysis of identified metabolites, and these metabolites could be enriched in 8 pathways (FDR < 0.05, impact > 2), including histidine metabolism, arginine biosynthesis, glutathione metabolism, cysteine and methionine metabolism, pantothenate and CoA biosynthesis, biotin metabolism, alanine, aspartate and glutamate metabolism, D-Glutamine and D-glutamate metabolism. These metabolic pathways are part of amino acid metabolism, carbohydrate metabolism as well as cofactor and vitamin metabolism. The bubble plot shown in **Fig. 3a** demonstrates the significance and the impact of each pathway. Figure 3b demonstrates the altered pathway sorted by impact factor from top to bottom. Figure 4a-b show metabolites in arginine biosynthesis and histidine metabolism. **Supplementary Figs. 2 and 3** demonstrate the details of the other 6 significantly altered pathways. More than 2 metabolites are identified in every pathway. Table 2 shows the FDR and the impact of enriched

pathways of altered metabolites of the patient's urine before and after CIRT. The alteration of arginine biosynthesis (Match status = 6/14) and histidine metabolism (Match status = 7/16) pathways by CIRT are the most significant, with an impact factor of 0.6 (FDR = 0.0093) and 0.5 (FDR = 0.0328), respectively. L-Glutamine, L-glutamate, L-Arginine, L-Citrulline, N-(L-Arginino)succinate, L-Ornithine in arginine biosynthesis are all downregulated (Fig. 4c), and L-Histidine, L-Glutamate, urocanate, N(pi)-Methyl-L-histidine, carnosine, imidazole-4-acetate in histidine metabolism are as well down-regulated (Fig. 4d).

Table 2
The FDR and impact of enriched pathways of altered metabolites between pre-CIRT samples and post-CIRT samples.

Pathway Name	Match Status	P	FDR	Impact
Alanine, aspartate and glutamate metabolism	5/28	0.003315	0.009313	0.33253
D-Glutamine and D-glutamate metabolism	2/6	0.003481	0.009313	0.5
Glutathione metabolism	5/28	0.003779	0.009313	0.30741
Cysteine and methionine metabolism	5/33	0.003834	0.009313	0.27873
Arginine biosynthesis	6/14	0.003835	0.009313	0.59898
Pantothenate and CoA biosynthesis	4/19	0.01807	0.032335	0.20714
Biotin metabolism	3/10	0.019576	0.032757	0.35
Histidine metabolism	7/16	0.020232	0.032757	0.52458

Metabolites profiles potentially to be a response indicator of CIRT

Moreover, the relation of metabolic clustering with different risk classification was further explored. According to the risk stratification, the low-risk and medium-risk patients were considered as a relatively low-risk group, and the high-risk and very high-risk patients were considered as a relatively high-risk group (Table 3).

Firstly, the metabolites of patients' pre-CIRT urine were further analyzed by PLS-DA and be well clustered into two groups and the results matched with the risk subtype (Fig. 5a). However, the PLS-DA analysis of post-CIRT urine metabolites shows more overlap (Fig. 5b), indicating patients assessed as the same risk subtype no longer represented similar metabolites profiles. This means CIRT could significantly decrease the discrimination of the risk stratification, indicating a possibility that CIRT could decrease the tumor heterogeneity.

Secondly, the HCA shows that after CIRT, the patients can be clustered into two groups according to the metabolites profiles of the patient's urine, named as PM1 and PM2 group (Fig. 5c). This clustering is

different from the risk subtype. PM2 group shows a higher concentration of urine metabolites than that of PM1 group, which means the patients in two groups may have different response to CIRT.

Table 3
Risk subtype of PCa patients.

risk group	n	risk subtype	n
Low	2	relatively low-risk	8
Intermediate	6		
High	5	relatively high-risk	6
Very high	1		

Discriminatory urine metabolites after CIRT mainly enriched in pathways of arginine biosynthesis and phenylalanine, tyrosine, and tryptophan biosynthesis

Pathway enrichment was further performed to show the response diversity of PCa to CIRT. Bubble chart of discriminatory metabolites is shown in **Fig. 6a**. Table 4 demonstrates the FDR and the impact of enriched pathways of discriminatory metabolites in post-CIRT urine samples. Discriminatory metabolites are mainly enriched in 8 pathways (FDR < 0.05, impact > 2), including phenylalanine, tyrosine and tryptophan biosynthesis, phenylalanine metabolism, biotin metabolism, cysteine and methionine metabolism, glutathione metabolism, arginine biosynthesis, alanine, aspartate and glutamate metabolism, D-Glutamine and D-glutamate metabolism. The difference of arginine biosynthesis pathway (Match status = 6/14), as well as phenylalanine, tyrosine and tryptophan biosynthesis (Match status = 1/4) pathway are the most significant, with an impact factor of 0.6 (FDR = 0.0261) and 0.5 (FDR = 0.0003) separately. Figure 6b demonstrates the concentration of L-Glutamine, L-glutamate, L-Arginine, L-Citrulline, N-(L-Arginino)succinate, L-Ornithine in arginine biosynthesis and L-Phenylalanine in phenylalanine, tyrosine and tryptophan biosynthesis are all higher in PM2 compared to PM1.

Table 4
The FDR and impact of enriched pathways of different metabolites between PM1 group and PM2 group

Pathway Name	Match Status	P	FDR	Impact
Phenylalanine, tyrosine and tryptophan biosynthesis	1/4	1.07E-05	2.67E-04	0.5
Phenylalanine metabolism	2/10	1.57E-05	2.67E-04	0.35714
Biotin metabolism	3/10	5.86E-04	0.004984	0.35
Cysteine and methionine metabolism	5/33	0.00615	0.026065	0.27873
Glutathione metabolism	5/28	0.009347	0.026065	0.30741
Arginine biosynthesis	6/14	0.009608	0.026065	0.59898
Alanine, aspartate and glutamate metabolism	5/28	0.009912	0.026065	0.33253
D-Glutamine and D-glutamate metabolism	2/6	0.013032	0.026065	0.5

Discussion

In this study, carbon ion showed its strong ability to inhibit the metabolism of prostate cancer. After CIRT treatment according to SOP in SPHIC, almost of the metabolites (33/35) were down-regulated. This result demonstrates the ability of CIRT treatment to inhibit the metabolism of tumors. Moreover, CIRT could generally inhibit most of the metabolism process, which will inhibit the proliferation, metastasis, and finally the progression of prostate cancer. Carbon ion is a novel tool for radiotherapy, and scarce studies revealed the influences of carbon ion on cancer metabolism, especially the prostate tumor. Although we don't have the data from photon radiotherapy, results in this study primarily suggest that one of the reasons for the strong inhibition effects of carbon ion on prostate cancer attribute to its ability to significantly down-regulate metabolism.

Herein, CIRT induced profiles changes of metabolites mainly enriched in arginine biosynthesis and histidine metabolism pathways, which were significantly inhibited by carbon ion. Arginine biosynthesis pathway played a key role and was up-regulated in the PCa progression [13, 14]. Arginine deprivation for the treatment of PCa has been investigated and proved effective [15]. Moreover, increased metabolism of L-arginine by myeloid cells can result in the impairment of lymphocyte responses to antigen during immune responses and tumor growth [16]. Thus, carbon ion induces such a high downregulation of arginine metabolism will benefit the inhibition of prostate cancer progression and have the potential to promote anti-tumor immune effects.

Interesting, we found the urine metabolites of these PCa patients have different response to CIRT treatment. And all of the patients could be clustered into two groups PM1 and PM2 after CIRT. PM2

showed relatively higher metabolites concentration. The clustered result was different from clinical risk stratification. Because the carbon ion will decrease metabolites of urine, herein the difference of metabolites concentration between PM1 and PM2 should attribute to the tumor sensitivity to carbon ion. PCa of PM2 group patients seems not that sensitive like PM1 group patients. Although we should wait for the follow-up result, it is still necessary to mention the importance of these results, which may have the potential to give a quick judgment of the treatment endpoint right after CIRT. Until now, there are no effective and powerful clinical tools to realize it.

Metabolomics results also showed the significant metabolites of CIRT response and enriched pathway showed that urine of PM2 group patients presented higher metabolites related to arginine biosynthesis as well as phenylalanine, tyrosine, and tryptophan biosynthesis. These results confirmed our result above, that arginine biosynthesis is important for PCa and maybe play a central role in carbon ion response. Arginine biosynthesis may be a promising indicator for individualized response of CIRT.

Conclusion

In this study, carbon ion showed its strong ability to inhibit almost of the metabolism pathways of PCa. CIRT induced changes of metabolites profiles mainly enriched in arginine biosynthesis and histidine metabolism. Urine metabolites of PCa patients had different response to CIRT treatment. More sensitive PCa showed lower level of metabolites in urine, especially the arginine biosynthesis as well as phenylalanine, tyrosine, and tryptophan biosynthesis pathway. Carbon-ion evoked metabolic programming seems to be one of the most important underlying mechanisms of CIRT to inhibit PCa. Urine metabolites also showed their potentials to identify the individualized response of PCa patients to CIRT radiotherapy. Due to the limitation of patient number, large amount investigation is needed.

Abbreviations

PCa: Prostate cancer; CIRT: Carbon ion radiotherapy; RFS: biochemical recurrence-free survival; SPHIC: Shanghai Proton and Heavy Ion Center; UPLC-MS/MS: high-performance liquid chromatography, coupled to tandem mass spectrometry; CTV: Clinical target volume; QC: Quality control; ESI: Electrospray ionization; FC: Fold change; FDR: False discovery rates; PCA: Principal component analysis; PLS-DA: Partial least-squares discriminant analysis; sPLS-DA: Sparse partial least-squares discriminant analysis; HCA: Hierarchical cluster analysis

Declarations

Ethics approval and consent to participate

This research had been approved by the institutional review boards of Shanghai proton and heavy ion center (SPHIC) and all patients provided written informed consent before admission.

Consent for publication

Not applicable.

Availability of data and materials

Data are available upon reasonable request to the corresponding author.

Competing interests

The authors declare no competing financial interests.

Funding

This article was supported by the Science and Technology Development Fund of Shanghai Pudong New Area (PKJ2019-Y07, PKJ2020-Y52, PKJ2019-Y06), the National Natural Science Foundation of China (21501029).

Authors’ contributions

YP, QZ and RN finished study design, QZ and YP finished experimental studies, YP and YS finished data analysis, QZ, PL, ZH, YP, WH and YD collected and proceeded patients samples and clinical information, YS, QZ and YP finished manuscript editing, QZ, XG and YS supervised the study. All authors read and approved the final manuscript.

Acknowledgements

We would like to acknowledge the reviewers for their helpful comments on this paper.

Authors' information

[1]Department of Radiation Oncology, Shanghai Proton and Heavy Ion Center, Fudan University Cancer Hospital, Shanghai 201321, China; [2]Department of Research and Development, Shanghai Proton and Heavy Ion Center, Fudan University Cancer Hospital, Shanghai 201321, China; [3]Department of Research and Development, Shanghai Proton and Heavy Ion Center, Shanghai 201321, China; [4]Department of Radiation Oncology, Shanghai Proton and Heavy Ion Center, Shanghai 201321, China;. [5]Shanghai Key Laboratory of Radiation Oncology (20dz2261000); [6]Shanghai Engineering Research Center of Proton and Heavy Ion Radiation Therapy, Shanghai 201321, China.

References

1. Nomiya T, Tsuji H, Kawamura H, Ohno T, Toyama S, Shioyama Y, et al. A multi-institutional analysis of prospective studies of carbon ion radiotherapy for prostate cancer: A report from the Japan Carbon ion Radiation Oncology Study Group (J-CROS). Radiother Oncol. 2016;121:288–93.
2. Zhang Y, Li P, Yu Q, Wu S, Chen X, Zhang Q, et al. Preliminary exploration of clinical factors affecting acute toxicity and quality of life after carbon ion therapy for prostate cancer. Radiat Oncol. 2019;14:94.
3. Peitzsch C, Gorodetska I, Klusa D, Shi Q, Alves TC, Pantel K, et al. Metabolic regulation of prostate cancer heterogeneity and plasticity. Semin Cancer Biol. 2020.
4. Chaiswing L, Weiss HL, Jayswal RD, Clair DKS, Kyprianou N. Profiles of Radioresistance Mechanisms in Prostate Cancer. Crit Rev Oncog. 2018;23:39–67.
5. Ng SSW, Jang GH, Kurland IJ, Qiu Y, Guha C, Dawson LA. Plasma metabolomic profiles in liver cancer patients following stereotactic body radiotherapy. EBioMedicine. 2020;59:102973.
6. Arenas M, Rodríguez E, García-Heredia A, Fernández-Arroyo S, Sabater S, Robaina R, et al. Metabolite normalization with local radiotherapy following breast tumor resection. PLoS One. 2018;13:e0207474.
7. Lindell Jonsson E, Erngren I, Engskog M, Haglöf J, Arvidsson T, Hedeland M, et al. Exploring Radiation Response in Two Head and Neck Squamous Carcinoma Cell Lines Through Metabolic Profiling. Front Oncol. 2019;9:825.
8. Dereziński P, Klupczynska A, Sawicki W, Pałka JA, Kokot ZJ. Amino Acid Profiles of Serum and Urine in Search for Prostate Cancer Biomarkers: a Pilot Study. Int J Med Sci. 2017;14:1–12.
9. Lima AR, Pinto J, Amaro F, Bastos ML, Carvalho M, Guedes de Pinho P. Advances and Perspectives in Prostate Cancer Biomarker Discovery in the Last 5 Years through Tissue and Urine Metabolomics. Metabolites. 2021;11:181.
10. Nalbantoglu S, Abu-Asab M, Suy S, Collins S, Amri H. Metabolomics-Based Biosignatures of Prostate Cancer in Patients Following Radiotherapy. Omics. 2019;23:214–23.
11. Cheema AK, Grindrod S, Zhong X, Jain S, Menon SS, Mehta KY, et al. Discovery of Metabolic Biomarkers Predicting Radiation Therapy Late Effects in Prostate Cancer Patients. Adv Exp Med Biol. 2019;1164:141–50.
12. Lee B, Mahmud I, Marchica J, Dereziński P, Qi F, Wang F, et al. Integrated RNA and metabolite profiling of urine liquid biopsies for prostate cancer biomarker discovery. Sci Rep. 2020;10:3716.
13. Qiu F, Huang J, Sui M. Targeting arginine metabolism pathway to treat arginine-dependent cancers. Cancer Lett. 2015;364:1–7.
14. Kelly RS, Vander Heiden MG, Giovannucci E, Mucci LA. Metabolomic Biomarkers of Prostate Cancer: Prediction, Diagnosis, Progression, Prognosis, and Recurrence. Cancer Epidemiol Biomarkers Prev. 2016;25:887–906.

15. Kim RH, Coates JM, Bowles TL, McNerney GP, Sutcliffe J, Jung JU, et al. Arginine deiminase as a novel therapy for prostate cancer induces autophagy and caspase-independent apoptosis. Cancer Res. 2009;69:700–8.
16. Bronte V, Zanovello P. Regulation of immune responses by L-arginine metabolism. Nat Rev Immunol. 2005;5:641–54.

Figures

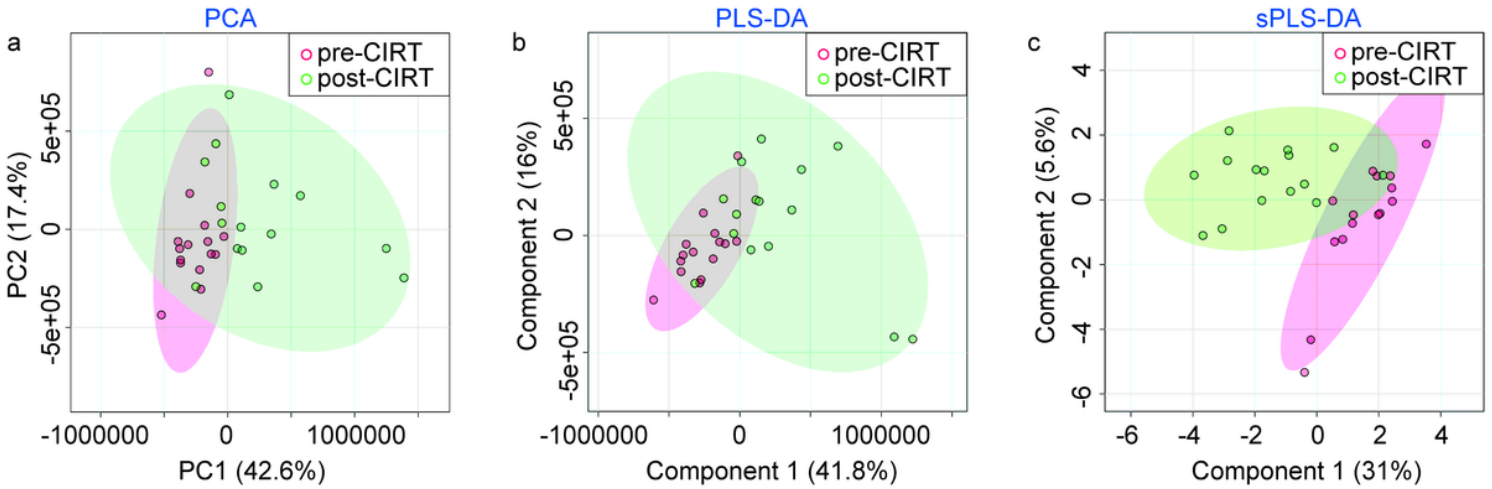

Figure 1

Multivariate statistical analyses of pre-CIRT (green) and post-CIRT (red) urine samples from PCa patients. a Principal component analysis (PCA) scores. b Partial least squares-discriminant analysis (PLS-DA). c Sparse partial least squares-discriminant analysis (sPLS-DA).

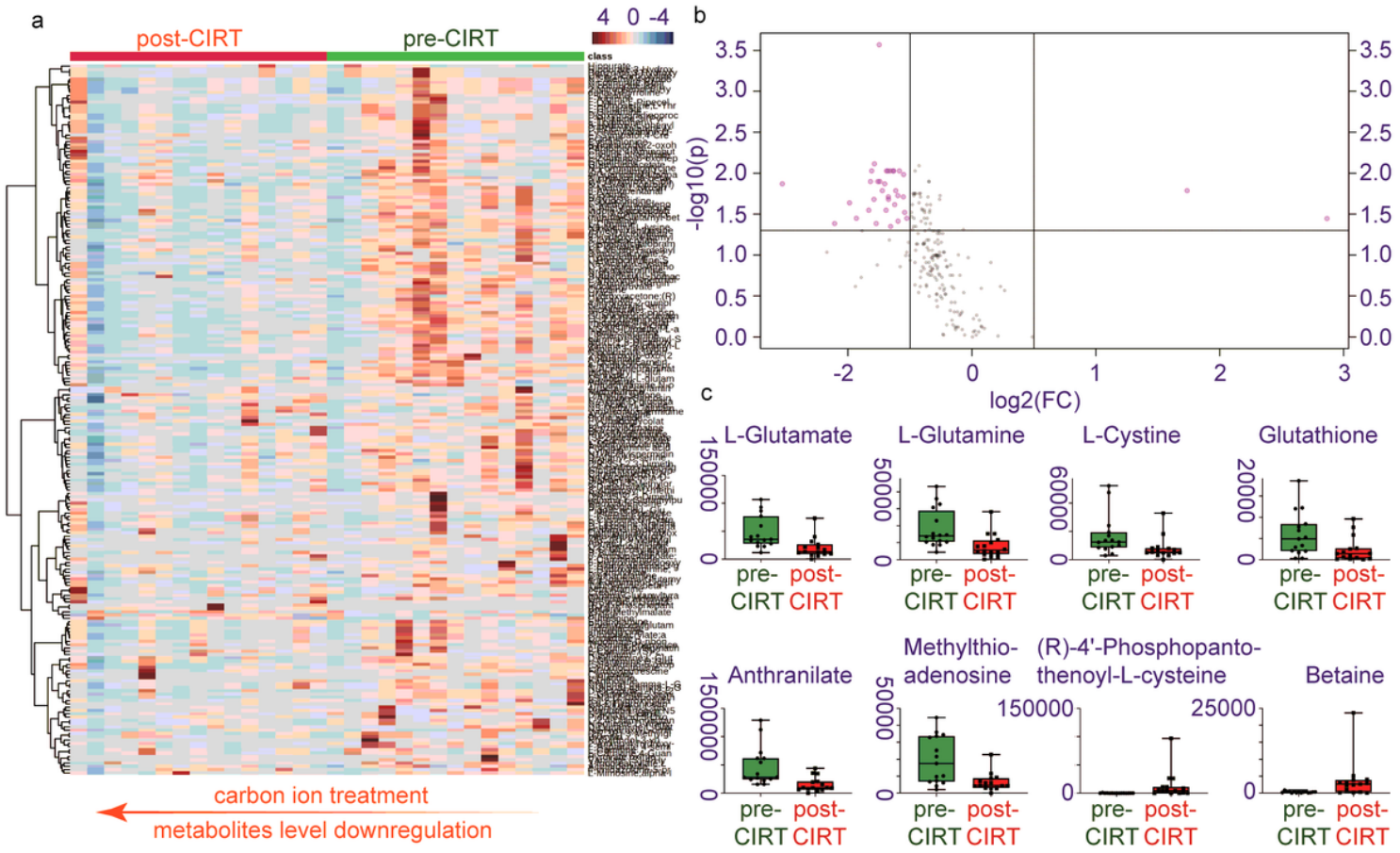

Figure 2

Metabolites profiles changes before and after CIRT. a Heat map based on concentration of metabolites in urine samples (n=30). Pre-CIRT samples are green (n=15) and post-CIRT samples are red (n=15). Up-regulated metabolites are shown in red and downregulated in blue. The intensity of the color estimates the magnitude of change. b Volcano plot of pre-CIRT samples and post-CIRT samples. Significant altered metabolites (FDR<0.05, fold change>2) are pink; non-significant altered metabolites are grey. c Boxplots demonstrate minimum, lower quartile, median, upper quartile, and maximum values of L-Glutamate, L-Glutamine, L-Cystine, glutathione, anthranilate, 5'-Methylthioadenosine, (R)-4'-Phosphopantothenoyl-L-cysteine, betaine; dots represent individual differences. Pre-CIRT samples are marked in green and post-CIRT samples are marked in red.

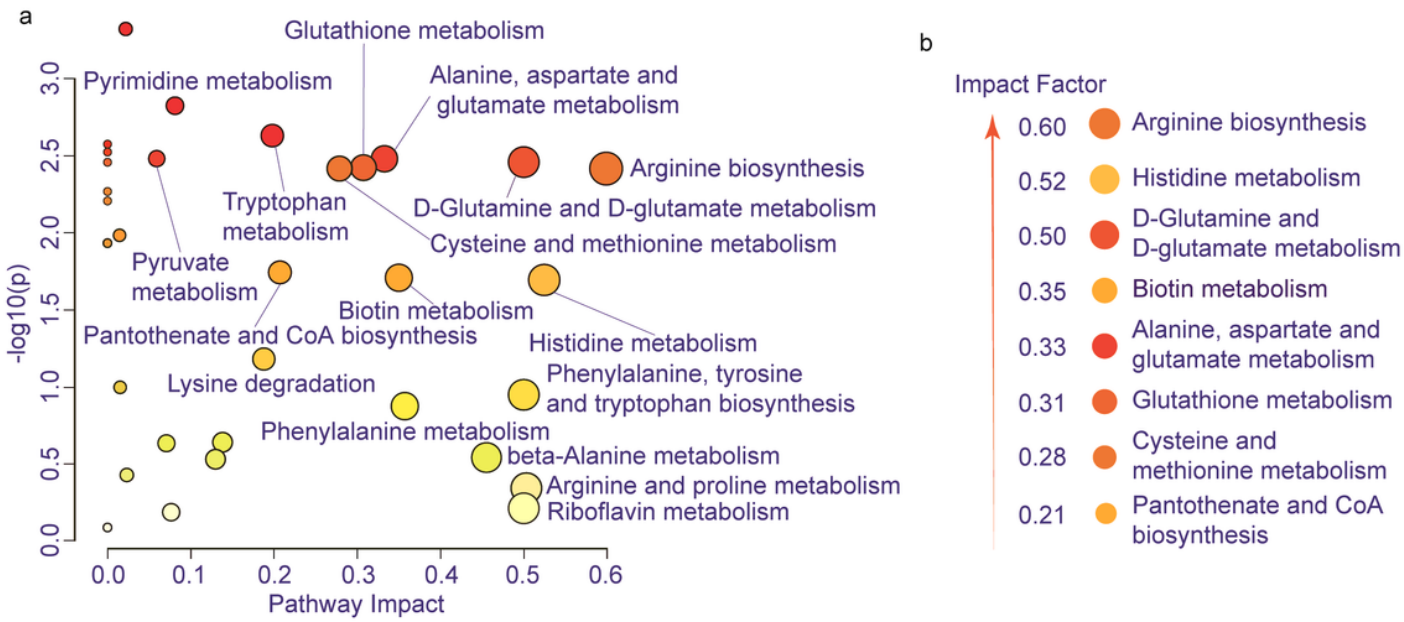

Figure 3

Metabolic pathway alteration by CIRT. a Bubble chart shows enrichment of metabolites altered pathways between pre-CIRT samples and post-CIRT samples. Y-axis label represents −log10(p) value, and X-axis label represents impact. Size and color of the bubbles represents the impact and −log10(p) values for each pathway obtained from enrichment pathway analysis. b Scheme shows the altered pathway sorted by impact factor from top to bottom.

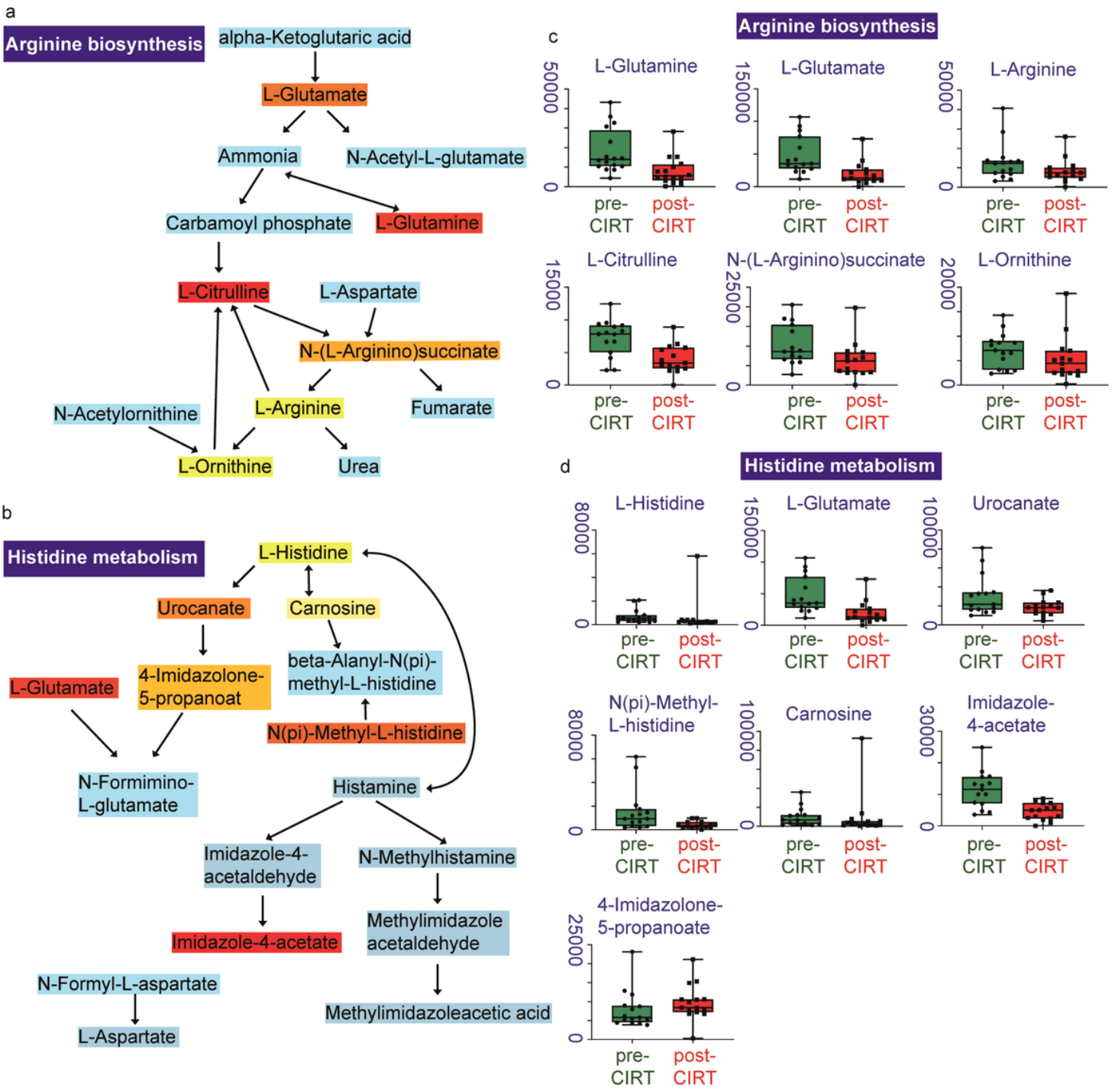

Figure 4

Altered metabolites in arginine biosynthesis and histidine metabolism pathways. Identified compounds within the pathway of arginine biosynthesis a and histidine metabolism b. Light blue means those metabolites are not in our data and are used as background for enrichment analysis; other colors (varying from yellow to red) means the metabolites are in the data with different levels of significance. Boxplots show minimum, lower quartile, median, upper quartile, and maximum values of L-Glutamine, L-glutamate, L-Arginine, L-Citrulline, N-(L-Arginino)succinate, L-Ornithine in arginine biosynthesis c, and L-Histidine, L-Glutamate, urocanate, N(pi)-Methyl-L-histidine, carnosine, imidazole-4-acetate, 4-Imidazolone-5-

propanoate in histidine metabolism d; dots represent individual differences. Pre-CIRT samples are marked in green and post-CIRT samples are marked in red.

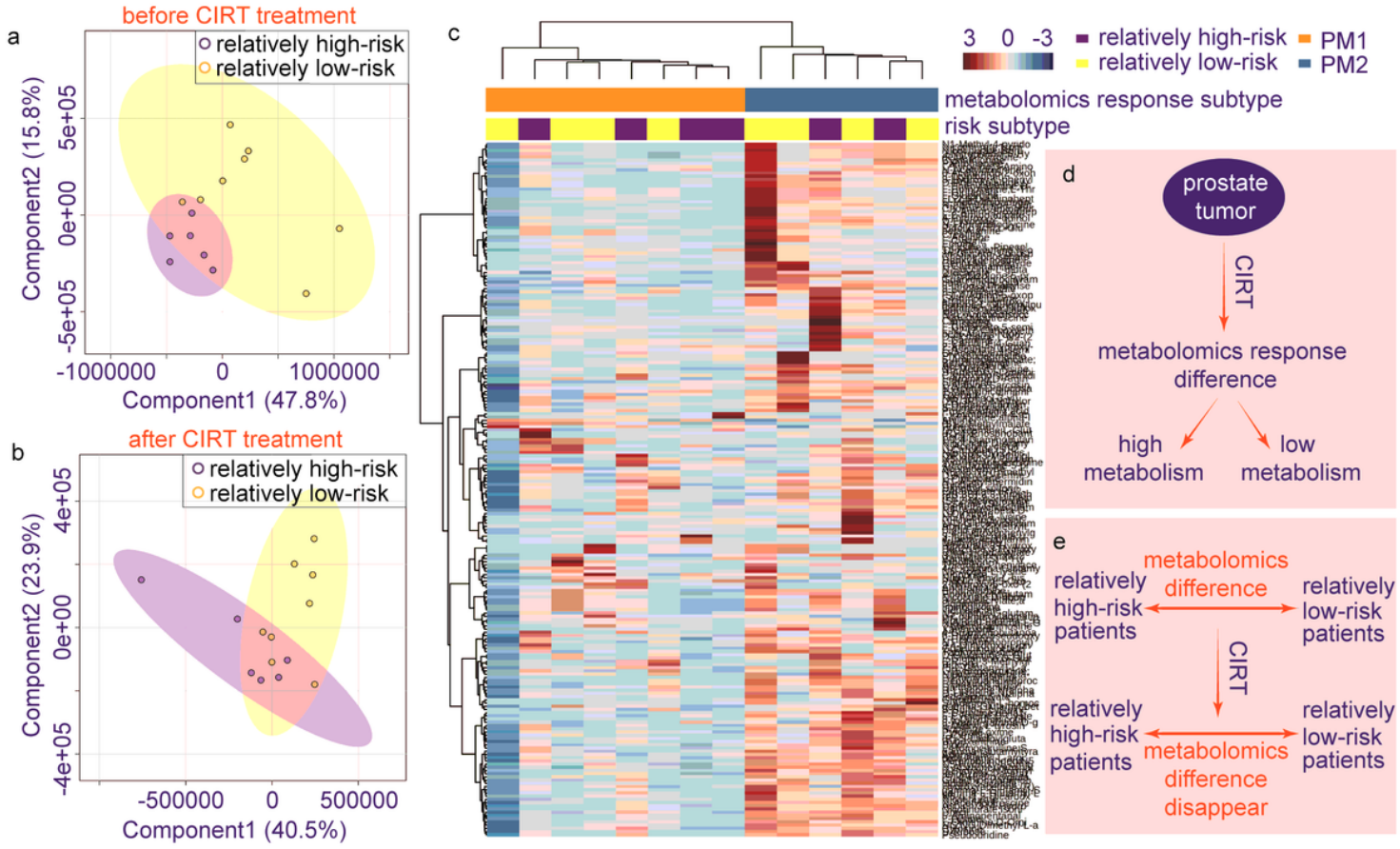

Figure 5

The individualized difference of metabolites profiles among patients after CIRT treatment. a PLS-DA analysis of relatively low-risk group (yellow) and the relatively high-risk group (purple) shows less overlap in pre-CIRT samples; b PLS-DA analysis of relatively low-risk group (yellow) and the relatively high-risk group (purple) shows less overlap in post-CIRT samples; c HCA of metabolites in post-treated samples. Risk subtype is demonstrated in yellow (relatively low-risk group) and purple (relatively high-risk group). Metabolomics response subtype is demonstrated in orange (PM1) and blue (PM2). Up-regulated metabolites are shown in red and down-regulated in blue. The intensity of the color estimates the magnitude of change. d Schematic description of individualized metabolomics response difference. e Schematic description of CIRT induced disappearance of metabolomics difference between relatively high-risk and low-risk patients.

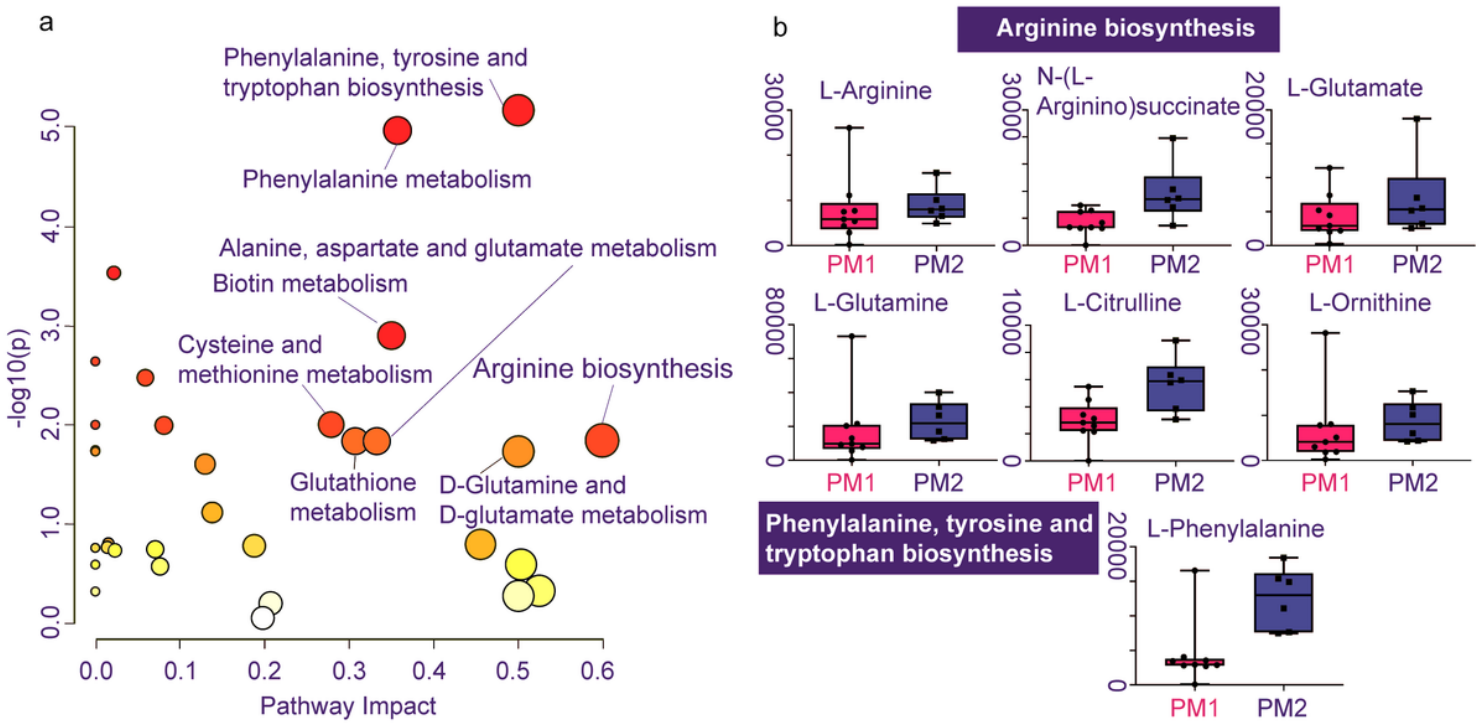

Figure 6

Individualized difference of response to CIRT treatment in metabolic pathways. a Bubble chart shows enrichment of metabolites altered pathways between pre-CIRT samples and post-CIRT samples. Y-axis label represents −log10(p) value, and X-axis label represents impact. Size and color of the bubble represent the impact and −log10(p) values for each pathway obtained from enrichment pathway analysis separately. b Boxplots show minimum, lower quartile, median, upper quartile, and maximum values of L-Glutamine, L-glutamate, L-Arginine, L-Citrulline, N-(L-Arginino)succinate, L-Ornithine in arginine biosynthesis and L-Phenylalanine in phenylalanine, tyrosine and tryptophan biosynthesis. PM1 samples are marked in pink and PM2 samples are marked in blue.

Supplementary Files

This is a list of supplementary files associated with this preprint. Click to download.

- Supplementaryinformation.docx